SF2A 2016
C. Reylé, J. Richard, L. Cambrésy, M. Deleuil, E. Pécontal, L. Tresse and I. Vauglin (eds)

SITELLE'S DATA RELEASE 1

T. B. Martin[1] and L. Drissen[1]

Abstract. Installed at the Canada-France-Hawaii Telescope (CFHT) since August 2015, SITELLE is an Imaging Fourier Transform Spectrometer (IFTS) with an 11×11 field of view. After its prototype SpIOMM, installed at Mont Mégantic (Québec, Canada), it is the second IFTS in the world operating in the visible band (350–1000 nm). It delivers hyperspectral data cubes of 4 million spectra at R∼1500–5000 with a spatial sampling of 0.32" and a filling factor of 100 %. A suite of softwares has been designed to reduce (ORBS) and analyze (ORCS) the data. Based on commissioning data obtained in August 2015, a first stable version has been released in March 2016 which is capable of reducing all the data. In this paper the quality of the calibration is discussed.

Keywords: SITELLE, SpIOMM, Imaging Fourier transform spectrometry, ORBS, ORCS, Data calibration

1 Introduction

Installed at the Canada-France-Hawaii Telescope (CFHT) since August 2015, SITELLE is an Imaging Fourier Transform Spectrometer (IFTS) with an 11×11 field of view. After its prototype SpIOMM (Drissen et al. 2008; Bernier et al. 2008), installed at Mont Mégantic (Québec, Canada), it is the second IFTS in the world operating in the visible band (350–1000 nm). It delivers hyperspectral data cubes of 4 million spectra at R∼1500–5000 with a spatial sampling of 0.32" and a filling factor of 100 %. The input light, modulated by a Michelson interferometer, is collected by two 2k×2k CCD cameras. A raw data set is composed of multiple couples of interferometric frames, one for each camera, taken at different position of the moving mirror. A suite of softwares has been designed to reduce (ORBS, Martin et al. 2012; Martin 2015) and analyze (ORCS, Martin et al. 2015, 2016) the data. Before the instrument's first light, ORBS was exclusively used to reduce the data of the prototype SpIOMM. Based on commissioning data obtained in August 2015 (Baril et al. 2016, Drissen et al., in preparation) and Science Verification data obtained in January 2016, a first stable version has been released in March 2016 which is capable of reducing all the obtained data with a first order calibration which will be enhanced in the next data release (Martin et al., in preparation). The quality of the calibration is going to be discussed in the next sections.

2 Instrumental line shape

The ideal instrumental line shape (ILS) of a phase corrected Fourier transform spectrum is a sinc. Any error in the phase correction may eventually result in a deformation of the ILS (e.g. Bell 1972) that will therefore generate wavelength and flux errors. When phase correction is possible, the attained level of precision of the phase correction is better than 1 percent for the relative pixel-to-pixel flux error and for the relative channel-to-channel flux error. Furthermore, no asymmetry of the instrumental line shape has been detected and its general model is very well described by our theoretical model (Martin et al. 2016).

3 Flux calibration

Flux calibration is based on the measurement of a spectrum of a spectrophotometric standard star every year in each filter. The obtained spectrum is used to correct for the wavelength dependant transmission of the

[1] Université Laval, 2325, rue de l'université, Québec (Québec), G1V 0A6, Canada

instrument and the telescope. A set of images of a standard star is also obtained at least once for each scan to get an accurate measurement of the mean sky transmission in the filter band. We have checked the accuracy of the flux calibration against various references: independant punctual sources (HETDEX Field, M1-71) and the integrated spectrum of a galaxy covering the whole field of view in three different filters (NGC 628, see Figure 1). All the results are reported in Table 1). There is an obvious general bias around -5 % which comes from the rough estimate of the modulation efficiency. A better estimate of the modulation efficiency can be derived from the ratio of the total spectral energy present in the output spectra and the total energy deposited by the photons in the input interferograms. It will be corrected in the next release. A conservative estimate of the precision of the flux calibration, i.e. without taking the bias into account, is around 5 %. The pixel-to-pixel precision of the flux calibration has been checked by comparing the Hα map of the planetary nebula M 57 obtained with SITELLE and the map obtained through the F656N filter of the Hubble Space Telescope (O'Dell et al. 2013). After a careful alignment and convolution of the HST map to respect SITELLE's pixel scale, an histogram of the flux ratio has been computed (see Figure 2). We can see that the error is smaller than 1.5% and the standard deviation of the ratios is smaller than 1.6%. Note that the object covers only a small part of the field of view (around 1×1 arcminute) so that general biases cannot be detected. A more careful testing with a larger object is required.

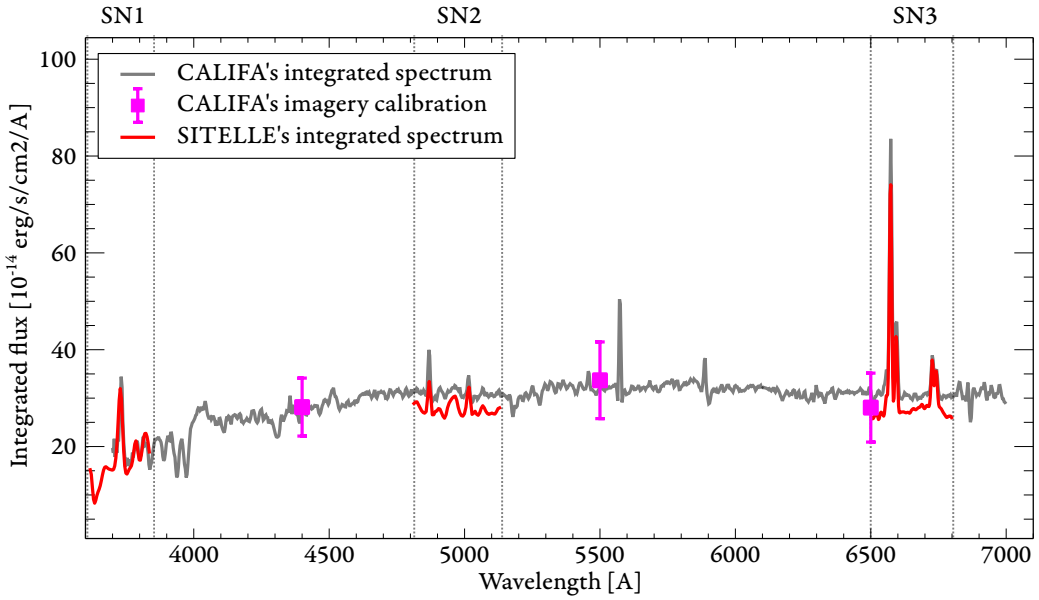

Fig. 1. Integrated spectrum of NGC 628 obtained with SITELLE in three filters (SN1, SN2 and SN3) superimposed on the integrated spectra obtained with PPaK (Sánchez et al. 2011; Kelz et al. 2006). SITELLE's spectra have been convoluted to respect PPaK's low resolution. A correction factor of 0.65 has been applied to consider PPaK's filling factor. The photometric calibration points used to calibrate PPAK spectrum are shown in purple along with their uncertainty. Part of the figure has been taken from Sánchez et al. (2011)

4 Wavelength calibration

A serious advantage of Fourier transform spectra when compared to any kind of dispersive technique is that the wavelength zero point is the only uncertainty. In other words there is no uncertainty on the relative wavelength calibration from one channel to the other. The observation of the light with an angle θ with respect to the axis of the interferometer translates in a position-dependant correction

$$\frac{\lambda_{\rm real}}{\lambda_{\rm obs}} = \cos(\theta) \ . \tag{4.1}$$

The zero point must therefore be calibrated for each spectrum of the cube. It is done via the observation of a laser source at Zenith. The deformation of the optical structure when the telescope moves from the Zenith position to the direction of the source is likely to produce an error in the relative wavelength calibration of up to

Table 1. Flux calibration check against various references. Three different filters have been checked: SN1 (362.6–385.6 nm), SN2 (482–513 nm) and SN3 (647.3–685.4 nm).

Object	Description	Error
NGC3344	Hα vs. SpIOMM	**-4%** ±2%
(Rousseau-Nepton et al.)	Hα + [NII]λ6584 vs. SpIOMM	**-4%** ±3%
M1-71	Hα vs Wright (2005)	**-7%** ±3%
	[NII]λ6584 vs Wright (2005)	**-11%** ±3%
NGC628	SN1 vs. CALIFA	**-6%** ±6%
	SN2 vs. CALIFA	**-7%** ±6%
	SN3 vs. CALIFA	**-9%** ±6%
HETDEX field	Lyα flux of $\sim$ 20 high redshift	**-5%**±7%
(Drissen et al.)	galaxies	

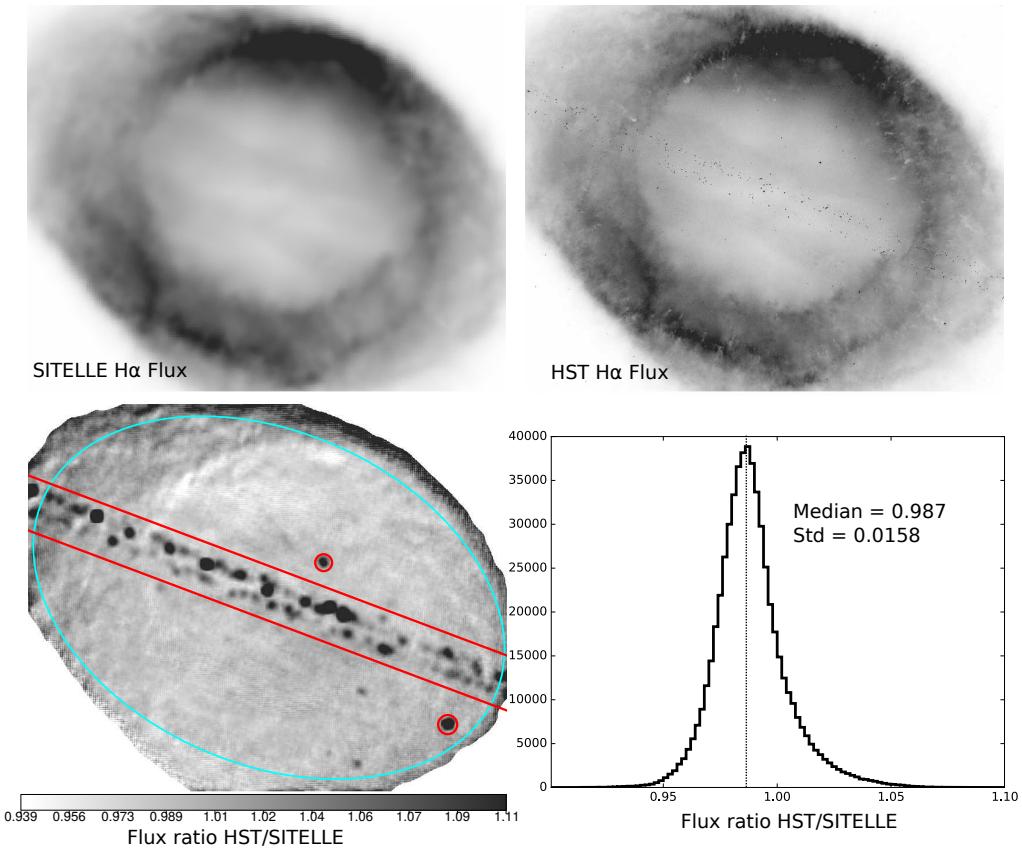

Fig. 2. Comparison of the Hα flux maps of the planetary nebula M 57 obtained with SITELLE (top-left) and the image obtained through the F656N filter with the Hubble Space Telescope (O'Dell et al. 2013, top-right). The bottom-left quadrant shows the pixel-to-pixel flux ratio and the bottom-right quadrant shows the histogram of the ratios. The HST map has been convoluted with a 8×8 kernel to fit the SITELLE's pixel scale. The regions shown in red have been excluded of the histogram because they are strong stars and reconstruction errors in the HST mosaic. The region included in the histogram is indicated as a blue ellipse.

15 km s^{-1}. The quality of the the calibration has been checked by comparing the velocity of 124 planetary nebulæ (PNe) detected with SITELLE in M 31, from a low resolution data cube obtained during the commissioning, with the velocity measured by Merrett et al. (2006). 86 of the 124 PNe show a compatible velocity within the uncertainties (see Figure 5). A much more precise checking has been obtained from the comparison of the velocity map of M 57 obtained with SITELLE versus the data obtained by O'Dell et al. (2007, 2013) with an Echelle spectrograph (Martin et al. 2016). Note that the original wavelength calibration of a cube (especially

in the SN3 red filter) can be improved to a precision of 0.3 km s^{-1} (at R=5000) by fitting the Meinel OH bands which are generally present everywhere in the cube (see Figure 3 and Figure 4). This operation can be done with ORCS.

Another source of absolute calibration uncertainty is the lack of precision on the calibration laser wavelength. The error on the velocity measurement is

$$\Delta v = c\frac{\Delta\lambda_{\mathrm{HeNe}}}{\lambda_{\mathrm{HeNe}}} \ . \tag{4.2}$$

Therefore an error of 1 Å on the calibration laser wavelength translates into an error of 55 km s^{-1}. This bias is easy to correct since the measurement of the Meinel OH bands in a few cubes is enough to get a better estimation. For the data release 1 we have used the manufacturer value of 543.5 nm which is biased by 80±5 km s^{-1}.

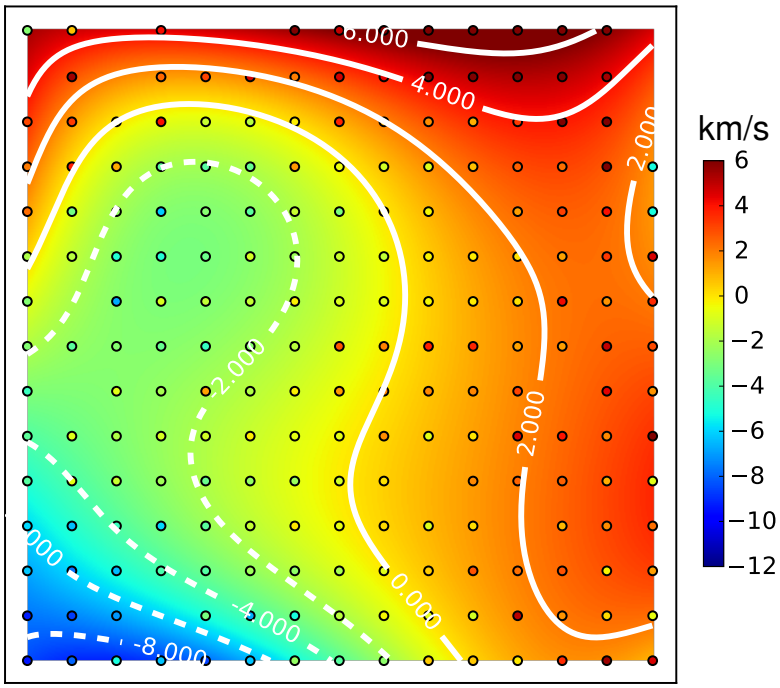

Fig. 3. Relative velocity map calculated from sky lines. Extracted from PG1216+069 in the SN3 filter at R=1900 (courtesy of Wei Hao Wang).

5 Astrometric calibration

Astrometric calibration is computed from the fit of the star-like sources detected in the field-of-view and the transformation of their celestial coordinates (Greisen & Calabretta 2002) found in the USNO-B1 catalog (Monet et al. 2003). The quality and the number of sources of the more recent Gaia data release 1 catalog has motivated its use for the next release instead of the old USNO catalog (Gaia Collaboration et al. 2016). The fitting engine fits all the stars at the same time which enhances the precision of the transformation parameters. The astrometric calibration is limited to 3 pixels (∼1") in an 11 arc-minutes circle around the center of the field by the optical distortions which are not taken into account in the present data release (see Figure 6).

6 Conclusions

We have discussed the calibration quality of SITELLE's first data release. We have shown that the absolute flux calibration was biased by -5% and that it was subject to a 5% variability from one observation to another. The general bias is likely to be corrected in the next release via a more precise estimation of the modulation efficiency. A ∼2 % pixel-to-pixel error is expected on the basis of a comparison with an Hubble images of M 57. The absolute wavelength calibration is also biased by 80±5 km s^{-1} due to the lack of precision on the calibration laser wavelength. The pixel-to-pixel error on the calibration can be as large as 15 km s^{-1} but it can be easily

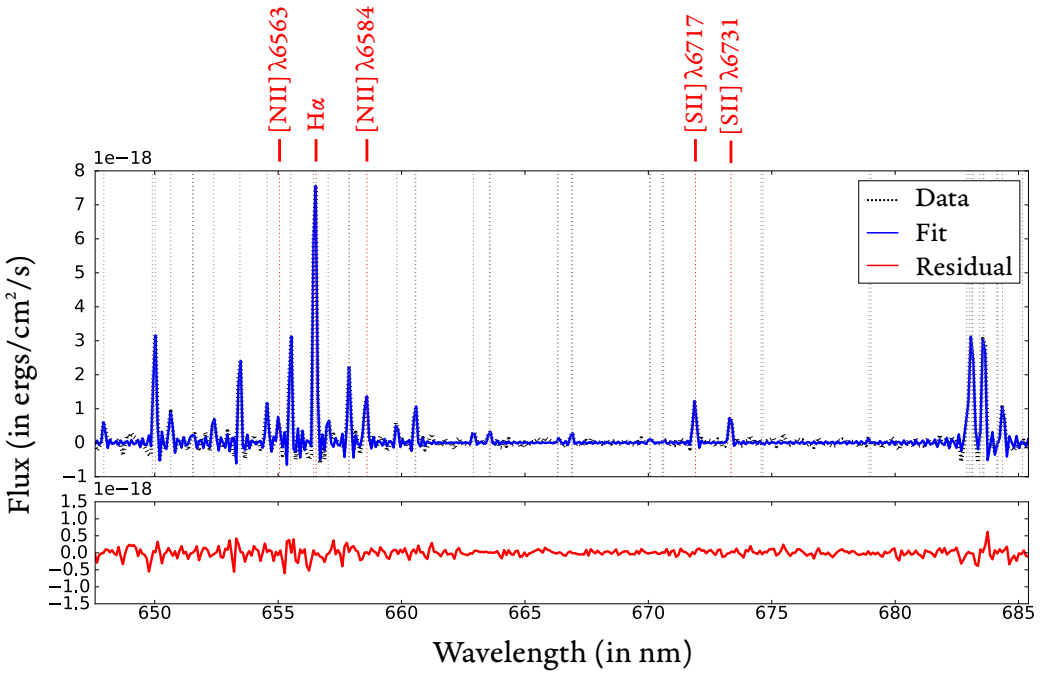

Fig. 4. Example of a fit of the Meinel OH bands of a sky spectrum in the field of IC 348. R = 4500 (courtesy of Gregory Herczeg). The fitted emission lines of the diffuse gas around the nebula are shown.

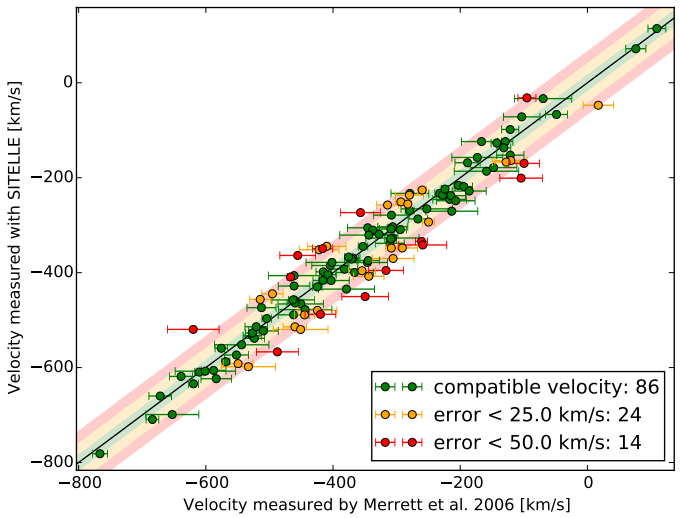

Fig. 5. Comparison of the measured velocity of 124 planetary nebulæ detected with SITELLE in M 31 with the measurement made by Merrett et al. (2006). The resolution of the cube is 400. The one-to-one line is indicated by a black line.

corrected by measuring the velocity of Meinel OH bands in the cube. This operation can be done with ORCS. The astrometric calibration is done via the comparison with the USNO-B1 catalog and is limited to ∼1" by the optical distortions which are not corrected in the present release. All the observed biases will be corrected in the next release. The precision on the pixel-to-pixel wavelength calibration will also be enhanced by the analysis of the internal phase of each cube that is directly related to the angle of the incident light and therefore to the velocity calibration (Martin et al., in preparation). The precision of the pixel-to-pixel flux calibration will also be enhanced by using a 3D phase correction and a better flatfield correction.

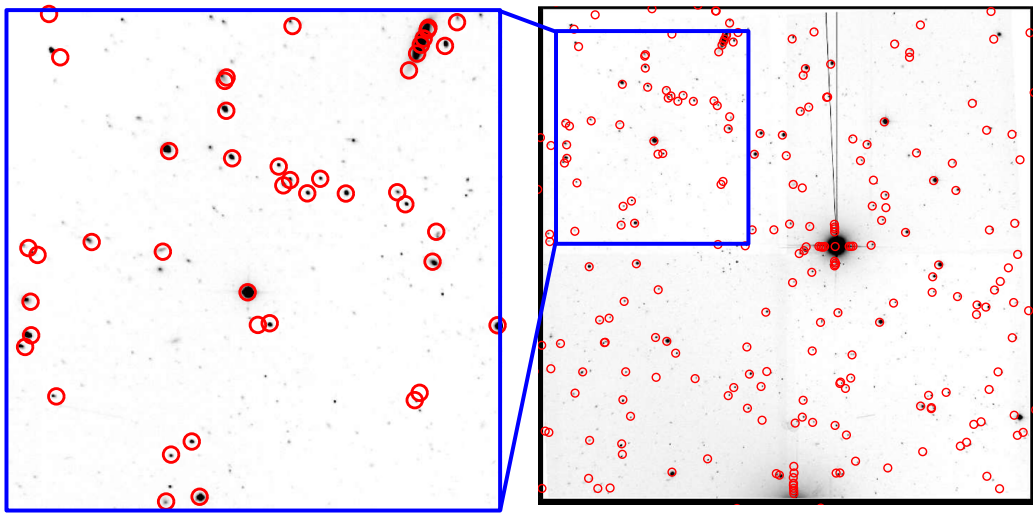

Fig. 6. Positions of the stars from the USNO-B1 catalog transformed with the computed World Coordinate System (WCS) of the field around the planetary nebula M1-71.

This paper is based on observations obtained with SITELLE, a joint project of Université Laval, ABB, Université de Montréal and the Canada-France-Hawaii Telescope (CFHT) which is operated by the National Research Council (NRC) of Canada, the Institut National des Science de l'Univers of the Centre National de la Recherche Scientifique (CNRS) of France, and the University of Hawaii. LD is grateful to the Natural Sciences and Engineering Research Council of Canada, the Fonds de Recherche du Québec, and the Canadian Foundation for Innovation for funding.

References

Baril, M. R., Grandmont, F. J., Mandar, J., et al. 2016, in Proc. SPIE, ed. C. J. Evans, L. Simard, & H. Takami (International Society for Optics and Photonics), 990829

Bell, R. J. 1972, Introductory Fourier transform spectroscopy (London: Academic Press)

Bernier, A.-P., Charlebois, M., Drissen, L., & Grandmont, F. 2008, in Proc. SPIE, Vol. 7014, Ground-based and Airborne Instrumentation for Astronomy II, 70147J

Drissen, L., Bernier, A.-P., Charlebois, M., et al. 2008, in Proc. SPIE, Vol. 7014, Ground-based and Airborne Instrumentation for Astronomy II, 70147K

Gaia Collaboration, Prusti, T., de Bruijne, J. H. J., et al. 2016, A&A, 595, A1

Greisen, E. W. & Calabretta, M. R. 2002, A&A, 395, 1061

Kelz, A., Verheijen, M. A. W., Roth, M. M., et al. 2006, PASP, 118, 129

Martin, T. 2015, Phd thesis, Université Laval

Martin, T., Drissen, L., & Joncas, G. 2012, in Proc. SPIE, Vol. 8451, Software and Cyberinfrastructure for Astronomy II, 84513K

Martin, T., Drissen, L., & Joncas, G. 2015, in PASP Conference Series, Vol. 495, Astronomical Data Analysis Software an Systems XXIV (ADASS XXIV), ed. A. R. Taylor & E. Rosolowsky, 327

Martin, T. B., Prunet, S., & Drissen, L. 2016, MNRAS, 463, 4223

Merrett, H. R., Merrifield, M. R., Douglas, N. G., et al. 2006, MNRAS, 369, 120

Monet, D. G., Levine, S. E., Canzian, B., et al. 2003, AJ, 125, 984

O'Dell, C. R., Ferland, G. J., Henney, W. J., & Peimbert, M. 2013, AJ, 145, 92

O'Dell, C. R., Sabbadin, F., & Henney, W. J. 2007, AJ, 134, 1679

Sánchez, S. F., Rosales-Ortega, F. F., Kennicutt, R. C., et al. 2011, MNRAS, 410, 313